2023, 20(3 Suppl.): 1146- 1154
https://dx.doi.org/10.21123/bsj.2023.7294
P-ISSN: 2078-8665 - E-ISSN: 2411-7986
Baghdad Science Journal

Synthesis and Evaluation of Platinum Nanoparticles Using *F. Carica* Fruit Extract and Their Antimicrobial Activities

Jenan Hussien Taha *[1], Nada Khudair Abbas [2] and Azhar A. F. Al- Attraqchi [3]

[1]Physiology and Medical Physics Department, College of Medicine, University of Al- Nahrain, Baghdad, Iraq
[2]Department of Physics, College of Science for Women, University of Baghdad, Baghdad, Iraq
[3]Department of Microbiology, College of Medicine, University of Al- Nahrain, Baghdad, Iraq
*Corresponding Author.

Received 06/04/2022, Revised 01/01/2023, Accepted 03/01/2023, Published 20/06/2023

Abstract

In this manuscript, a simple new method for the green synthesis of platinum nanoparticles (Pt NPs) utilizing F. carica Fig extract as reducing agent for antimicrobial activities was reported. Simultaneously, the microstructural and morphological features of the synthesized Pt NPs were thoroughly investigated. In particular, the attained Pt NPs exhibited spherical shape with diameter range of 5-30 nm and root mean square of 9.48 nm using Transmission Electron Microscopy (TEM) and Atomic Force Microscopy (AFM), respectively. Additionally, the final product (Pt NPs) was screened as antifungal and antibacterial agent against Candida and Aspergillus species as well as Gram-positive Staphyllococcus aureus and Gram-negative Acinetobacter species, respectively. Accordingly, the synthesized NPs demonstrated inhibition zones of 36 and 28 mm against fungal and bacterial species, respectively. The presented Pt NPs play an active role in both antifungal and antibacterial activities which indicates the presence of a well-regulated nano-materials system for biomedical application.

Keywords: *antibacterial, antifungal, F. carica extract*, Green synthesis, Pt NPs.

Introduction

Metal and metal oxide NPs are of obvious interest among researchers because of their distinctive features including easy separation, low toxicity, and significant surface-to-volume ratio[1,2]. Metal and metal oxide NPs have shown a wide-range of applications such as solar cells, sensors, thermoelectric, catalysis…etc.[3-7]. In the field of nanotechnology, nanomedicine in particular, metal and metal oxide have revealed promising properties as antimicrobial agents [8, 9].

Pt NPs have revealed considerably superior role in humans compared to cisplatin, which is a cancer medication[10,11]. Pt NPs attracted a significant attention owing to their outstanding performance as antimicrobial agent [12]; This could be attributed to a number of reasons; for instance, because of their relatively small size, considerable surface area, biocompatibility as well as low toxicity. The aforementioned features permit the Pt NPs to penetrate bacteria and fungi living-cell membranes which in turn result in an anticipated influence of intracellular mechanisms[12-16]. The considerable activity of Pt NPs is also attributed to relatively excessive cellular uptake, yet in vivo reduction alters the pharmacological features and subsequently drug efficiency. The potential benefit of Pt NPs is the comparatively low reactivity which results in lower loss of the active drug as well as reduces the undesired reactions[10,17]. Moreover, due to the increase of environmental concerns initiated through the chemical and physical approaches, efforts are being conducted in order to develop NPs synthesis techniques using natural resources. In this attempt, several techniques were conducted in order to synthesize a well-oriented Pt NPs for the sole

2023, 20(3 Suppl.): 1146- 1154
https://dx.doi.org/10.21123/bsj.2023.7294
P-ISSN: 2078-8665 - E-ISSN: 2411-7986
Baghdad Science Journal

purpose of inhibiting the bacterial/fungal growth [18-21]. The green synthesis approaches involving the utilization of enzymes, plants extracts, as well as microorganisms play a vital role in the environmentally friendly Pt NPS formation[22- 24].

Therefore, this study aims to demonstrate the synthesis of Pt NPs utilizing *F. carica* (common Figs) extract as a reducing agent. The structural, morphological, and optical properties of the attained product are demonstrated in detail. Furthermore, the synthesized Pt NPs are assessed for antifungal activity using *Candida* and *Aspergillus* species alongside the antibacterial activity against Gram-positive *Staphyllococcus aureus* and Gram-negative *Acinetobacter* species.

Materials and Methods

Experimental Procedures

1. Plant collection and extraction

Dried *carica* Figs were acquired from a local market in Baghdad, Iraq. The collected fruit was washed thoroughly and 20 gm of the fruit were ground and blended alongside 100 ml of distilled-deionized water (DDW). The solution was later heated to 100 °C in a closed flask and subsequently cooled down to room temperature (RT) for one hour [25]. Finally, the mixture was filtered using chromatography paper (Whatman No.1) then incubated at RT for additional use.

2. Synthesis of Pt NPs

The experimental procedure of Pt NPs synthesis consists of specific amount 0.5, 1, and 2 mM of Chloroplantinic acid (H_2PtCl_6. $6H_2O$) as precursor under a stirring rate of 600 rpm for 20 minutes at 30 °C. Afterwards, the Fig extract was added to the mixture with molar ratio of 1:9 in 10 mL DDW under stirring rate of 400 rpm for 3 hours at 50 °C. Subsequently, the resultant mixture was centrifuged for 30 minutes at 4000 rpm; and the residue was washed with multi-cycle centrifugation procedure. Hereinafter, the precipitate was dried at 75°C in an oven for 8 hours. Finally, the Pt NPs samples were denoted as Pt NPs-1, Pt NPs-2, and Pt NPs-3 for 0.5, 1, and 2 mM, respectively.

3. Characterization

The microstructural features of the prepared NPs were studied via Shimadzu X-ray Diffractometer (XRD-6000) with wavelength of 1.541 A° and Cu-Kα radiation. In the meanwhile, compact char surface was investigated using Fourier Transform Infrared Spectroscopy (FTIR, Thermo Nicolet Nexus) ranging from 400 to 4000 cm^{-1}. Furthermore, the optical investigation of the obtained Pt NPs was performed via Shimadzu UV-1800 UV-Vis spectrophotometer. Atomic Force Microscopy (SPM AA3000-AFM) and TECNAI F-30 TEM were used for the morphological and nanoparticle size investigations.

4. Antimicrobial Activities

The antifungal and antibacterial activities of Pt NPs were evaluated using the well-known agar well diffusion method[26]. Herein, the antifungal activity was screened against *Candida* and *Aspergillus* species, whereas, the antibacterial activity was monitored against Gram-positive *Staphylococcus aureus* and Gram-negative *Acinetobacter* species. In a typical procedure, the agar petri dish was thoroughly swabbed with sterile cotton swap technique in which 30 ml of 24 hours Sabouraud′s dextrose and blood agar were used for each fungal and bacterial species. Continuously, wells were made in the pre-solidified agar plates via 5 mm cork bor-er. Variety of Pt NPs concentrations 37.5, 75, 150, 300, 600 and 1200 µg/ml were employed in order to estimate the synthesized NPs antifungal activities. Concurrently, the antibacterial activity was performed using Pt NPs with concentrations of 50,100,200, 300, 400 and 500 µg/ml. Finally, the antimicrobial activity, in general, was recorded after incubation time of 24 hours. It is worth mentioning that DDW was utilized as negative control while standard antibiotics was employed as positive control.

Results and discussion

1. Structural analysis of Pt NPs

Figure 1 a illustrates the X-ray diffractions analysis of the synthesized Pt NPs. Three pronounced peaks, shown in Fig. 1 a, were acquired at around 2θ = 38.7°, 45.2°, and 67.9° which corresponds to the lattice reflections of the (111), (200), and (220) planes for 2mM, 1mM, and 0.5mM, respectively. This observation confirms the crystal structure formation of Pt NPs (JCPDS-No: 38–0486) [27, 28]. The intensity of the XRD peak was noticed to be slightly increased as a function of the utilized concentration and more intensity at concentration 1mM. Crystallite size was calculated in accordance with Debye-Scherrer's formula[29], the corresponding outcomes

2023, 20(3 Suppl.): 1146- 1154
https://dx.doi.org/10.21123/bsj.2023.7294
P-ISSN: 2078-8665 - E-ISSN: 2411-7986
Baghdad Science Journal

are demonstrated in Fig. 1 b. It is an established fact that the FWHM can be used as a crystal quality indicator according to Debye-Scherrer's model; thereby higher crystal quality exhibits low FWHM[30]. Hence, as illustrated in Fig. 1 b, it is evident that the crystal quality of the acquired Pt NPs for the prepared samples reached the highest value at around 1 mM molar. Fig. 1 c, illustrates the FTIR spectrum obtained for Pt NPs clearly shows O-H stretching bond at 3440.21 cm^{-1}, while other characteristic peaks at 2899.73 and 2330.29 which correspond to both $C-H$ and $C \equiv N$ stretching vibrations, respectively. Moreover, the occurrence of characteristic peaks at 2067 and 2042 cm^{-1} are attributed to the Pt-Pt bond stretching which agrees well with the literature[31]. The Pt amine vibration was noticed at 1645.04 cm^{-1} and peaks at 1061 and 1437.53 cm^{-1} are due to the $C-O$ and $C=C$ stretching, respectively. Finally, characteristic peak at around 800.51 cm^{-1} are designated to the surface atoms complexation process[31, 32].

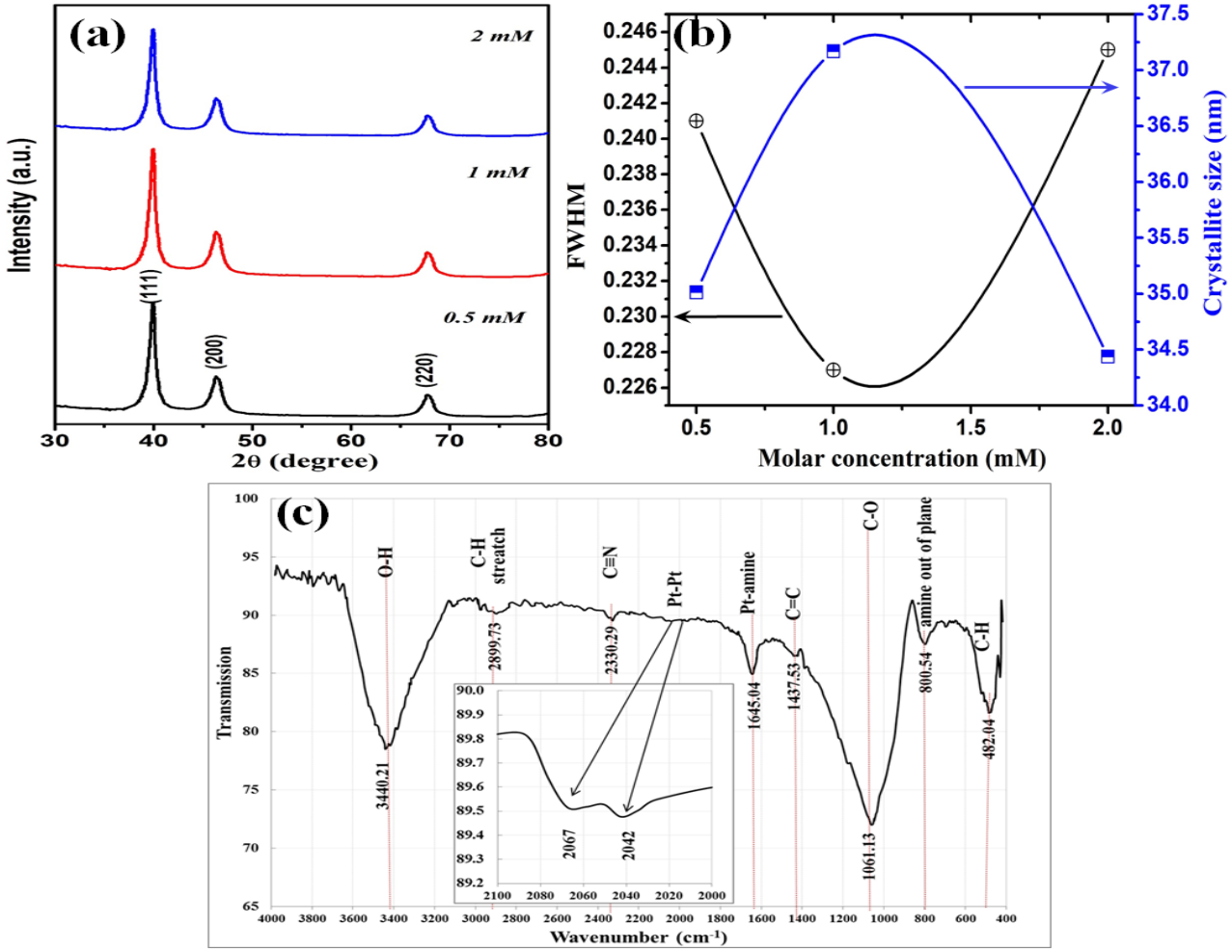

Figure 1.(a) XRD patterns of Pt NPs, (b) FWHM and crystallite size of Pt NPs, and (c) FT-IR spectrum of 1 mM Pt NPs.

2. Optical analysis of Pt NPs

Fig.2 a illustrates the UV-Vis spectra of the presented Pt NPs at different concentrations, by which a cut-off phenomenon was noticed at around 350 m. The latter was originated from the direct transition of the Pt NPS, with respect to the employed concentrations. Simultaneously, the optical band gaps were calculated via Tauc relation, the Tauc relation is used to extract the optical band gap (Eg) of the sample based on its mathematical relation with absorption coefficient (α) and hv is a photon energy, as represented in the equation below[33]

$$(\alpha hv)^2 = A(hv - E_g),$$

2023, 20(3 Suppl.): 1146- 1154
https://dx.doi.org/10.21123/bsj.2023.7294
P-ISSN: 2078-8665 - E-ISSN: 2411-7986
Baghdad Science Journal

as elucidated in Fig. 2 b. The evaluated optical band gaps exhibited almost similar values in which it is verified that the utilized molar concentrations have relatively low effect on the optical properties of the synthesized NPs. The obtained findings are in good agreement with the crystallite size obtained through XRD analysis.

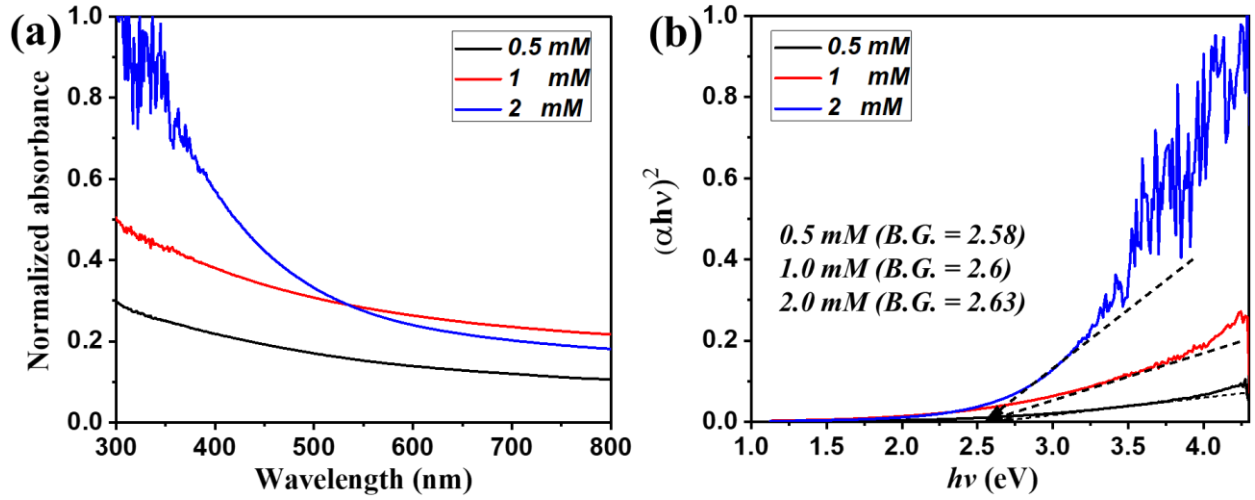

Figure 2. (a) Optical absorption and (b) optical band gap of the synthesized PT NPs.

3. Morphological Analysis of Pt NPs

The AFM two- and three-dimensional illustrations with scanning area of $2\mu m$ are depicted in Fig. 3 a. It is evident that the synthesized NPs are vertically aligned with spherical shape. Additionally, the average RMS and surface roughness exhibited values of 9.48 and 8.28 nm, respectively, while the average diameter was found to be 49.46 nm. The former suggests the occurrence of rough surface that in turn leads to high electrochemical performance[34]. Subsequently, the prepared NPs morphological properties were also studied through TEM analysis, as displayed in Fig. 3 a. Within the TEM analysis, it was observed that the attained Pt NPs demonstrated a particle diameter ranging from 5 to 30nm, whereby the average diameter was found to be 16 nm. The upper limit of the particle diameter was found to be relatively close to the diameter acquired in the AFM analysis Fig. 3 a.

2023, 20(3 Suppl.): 1146- 1154
https://dx.doi.org/10.21123/bsj.2023.7294
P-ISSN: 2078-8665 - E-ISSN: 2411-7986
Baghdad Science Journal

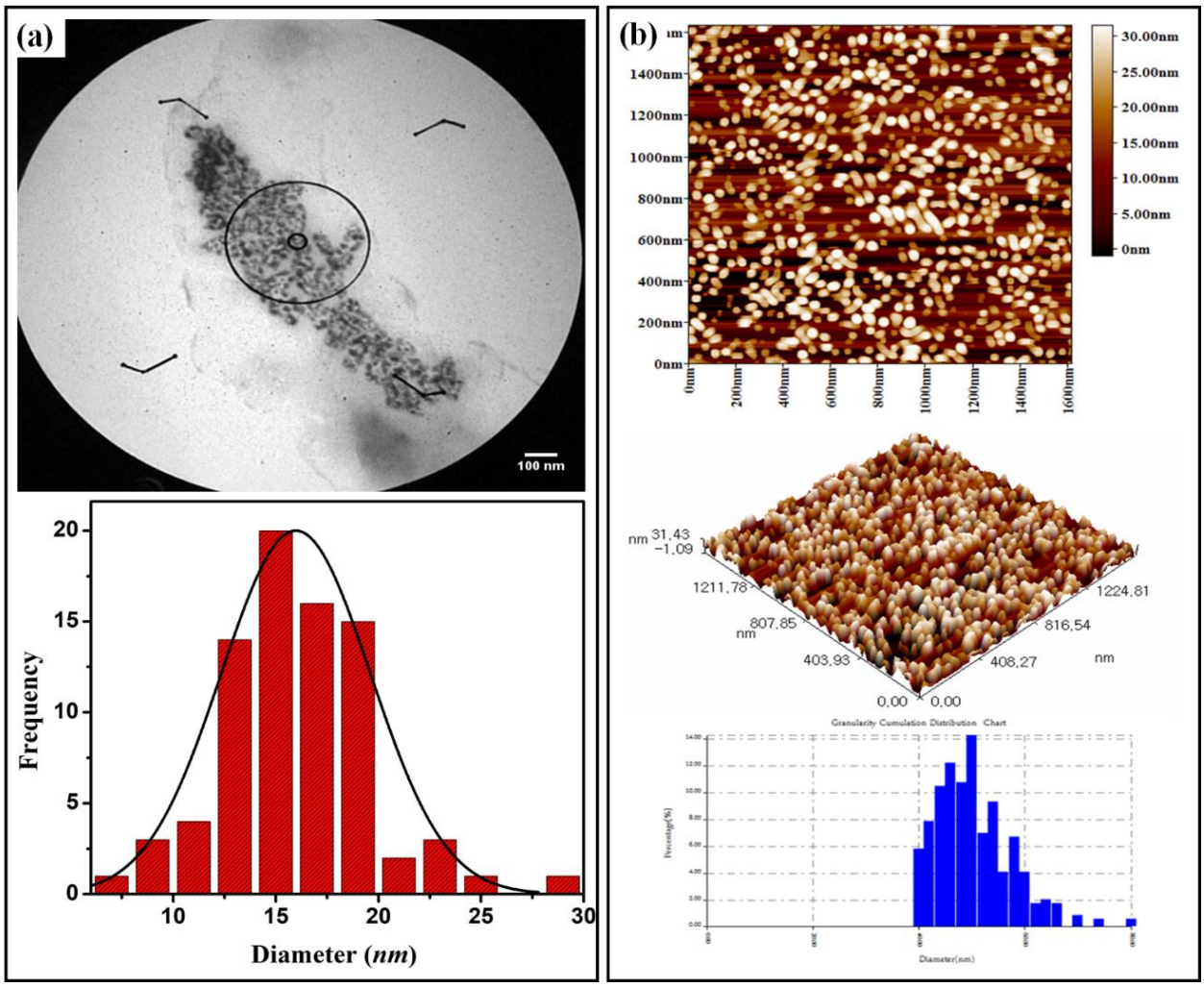

Figure 3. (a) TEM image and, (b) 2D and 3D illustration AFM of the synthesized Pt NPs.

4. Antimicrobial Analysis of Pt NPs

The antimicrobial activities of the green synthesized Pt NPs are demonstrated in Fig. 4 a and b. Generally, it is established that the fungal and bacterial cells' size range within micrometer scale; in the meanwhile, these cells contain pores in the micrometer scale. Henceforth, NPs with size scale comparable to the pores possess a unique property in which a clear passage to the cell membrane might be attained[35, 36]. As shown in Fig. 4 a, Pt NPs exhibited an increase zone of inhibition with the increment of the NPs concentrations against both *Candida* and *Aspergillus* fungi species. Pt NPs exhibited higher inhibition zone against *Aspergillus* species. than *Candida* spp. The stated observation was only noticed at low NPs concentrations 75 and 150 µg/ml. However, the inhibition zone in the case of *Candida* spp. was noticed to be higher at greater NPs concentrations. In details, concentration as low as 75 µg/ml revealed inhibition zones of 11.5 and 11*mm* in the case of *Aspergillus* and *Candida*, respectively. Inversely, inhibition zones of 28, 31 *mm* were monitored against *Aspergillus* and *Candida* at NPs concentration of 600 µg/ml as shown in Fig 5 a and b, respectively. Table. 1, shows the antifungal activity using standard antibiotics in which it can be clearly indicated that proposed nanomaterials system has an active role against the utilized fungi spp. as compared to the standard antibiotics.

2023, 20(3 Suppl.): 1146- 1154
https://dx.doi.org/10.21123/bsj.2023.7294
P-ISSN: 2078-8665 - E-ISSN: 2411-7986
Baghdad Science Journal

Table 1. Zone of inhibition diameters of antifungal in comparison with the Pt NPs and DDW for *Candida* Spp. and *Aspergillus* Spp.

fungal	minimum inhibition zone (mm)					
	KCA (10 µg)	NY (100un)	AMB (20µg)	FCN (10µg)	DDW	platinum NPs (75 µg)
candida spp.	35	14	11.4	23	0	12
Aspergillus spp.	21	17.2	12	0	0	11

KCA: Ketoconazole NY: Nystatin
AMB: Amphotericin-B FCN: Fluconazole

Similarly, the Pt NPs antibacterial activity against two bacteria spp. was tested using Gram-positive *S. aureus* and Gram-negative *Acinetobacter* spp at different Pt NPs concentrations. The outcomes of this investigation can be seen in Fig. 4 b. Herein, a comparable behavior to the antifungal activity was observed in which a growth in the zone of inhibition was perceived alongside the NPs concentration increment. NPs concentration of 100 µg/ml showed inhibition zones of 11 and 9 *mm* against Gram-positive *S. aureus* and Gram-negative *Acinetobacter* spp, respectively. Whereas inhibition zones of 28 and 24 µg/ml were detected using NPs concentration of 500 µg/ml for Gram-positive *S. aureus* and Gram-negative *Acinetobacter* spp as in Fig 5 c and d, respectively. Besides, the acquired antibacterial activity was compared to those obtained using standard antibiotics, the relevant results are presented in Table. 2. Hereinafter, the demonstrated outcomes suggest that the utilized Pt NPs exhibited an active role in killing/inhibiting both fungi and bacteria growth.

Table 2. Zone of inhibition diameters of antibacterial in comparison with Pt NPs and DDW for *Staphyllococcus aureus* Spp. and *Acinetobacter* Spp.

bacterial isolates	minimum inhibition zone (mm)								
	CRO (30 µg)	AK (30µg)	SAM (20µg)	TS (25µg)	CD (2µg)	CIP (5µg)	ATH (15µg)	DDW	Platinum NPs (100 µg)
S. aureus	25	18	15	13	0	0	0	0	11
Acinetobacter baumanii	0	0	0	0	0	0	0	0	10.8

CRO: Ceftriaxone AK: Amikacin SAM: Ampicilin + Sulbactam
TS: Trimethoprim CD: Clindamycin CIP: Ciprofloxacin ATH: Azithromycin

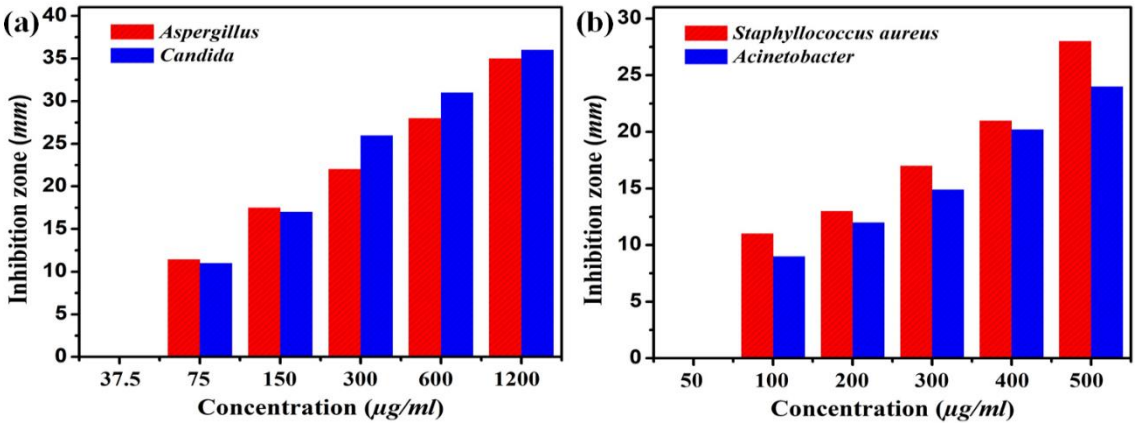

Figure 4. Inhibition zones of Pt NPs: (a) fungi and (b) bacteria.

2023, 20(3 Suppl.): 1146- 1154
https://dx.doi.org/10.21123/bsj.2023.7294
P-ISSN: 2078-8665 - E-ISSN: 2411-7986
Baghdad Science Journal

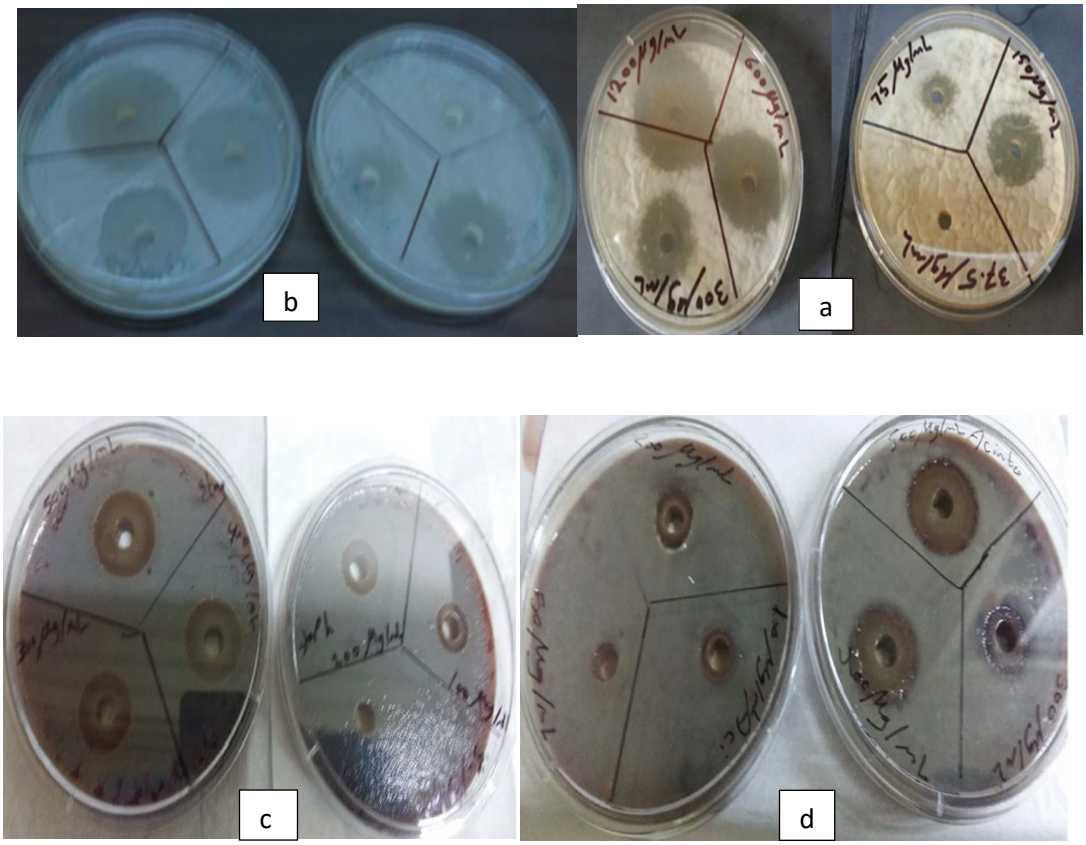

Figure 5. Images for the zone of inhibition by Pt NPs (a) Candida Spp, (b)Aspergillus Spp, (c) S. aureus Spp, and (d) Acinetobacter Spp

Conclusion

A simple pathway for the green synthesis of Pt NPs utilizing *F. carica* Fig extract was effectively demonstrated. The attained Pt NPs were characterized using variety of analytical techniques in which average particle diameter and RMS values of 16 and 9.48 *nm* were acquired using TEM and AFM techniques, respectively. Furthermore, the antimicrobial activities were also studied against two types of fungi and bacteria species. The antifungal activity seemingly found with developed role in capturing the species in comparison with the antibacterial activity, with respect to the used Pt NPs concentrations. The highest zone of inhibition was found to be 36 *mm* in the case of *Candida* spp as compared to 28 mm inhibition zone against Gram-positive *S. aureus*.

Author's Declaration

- Conflicts of Interest: None.
- We hereby confirm that all the Figures and Tables in the manuscript are ours. Furthermore, any Figures and images that are not ours have been included with the necessary permission for re-publication, which is attached to the manuscript.
- Ethical Clearance: The project was approved by the local ethical committee in University of Al-Nahrain.

Author's Contribution Statement

J. H. T. and N. K. A. conceived of the presented idea. J. H. T., N. K. A. and A. A. F. developed the theory and verified the analytical methods. N. K.A. and A. A. F. supervised the findings of this work. A A.F. wrote the manuscript. All authors discussed the results and contributed to the final manuscript.

2023, 20(3 Suppl.): 1146- 1154
https://dx.doi.org/10.21123/bsj.2023.7294
P-ISSN: 2078-8665 - E-ISSN: 2411-7986
Baghdad Science Journal

References

1. Salih, E. Y., Bashir, M. B. A., Rajpar, A. H., Badruddin, I. A., & Bahmanrokh, G. (2022). Rapid fabrication of NiO/porous Si film for ultra-violate photodetector: The effect of laser energy. Microelectronic Engineering, 258, 111758.
2. Razzaque S, Hussain S Z, Hussain I, Tan B. Design and utility of metal/metal oxide nanoparticles mediated by thioether end-functionalized polymeric ligands. Polymer. 2016; 8: 156.
3. Yun S, Hagfeldt A, Ma T. Pt-free counter electrode for dye-sensitized solar cells with high efficiency. Adv Mater. 2014; 26: 6210-6237.
4. Ding K, Gulec A, Johnson A M, Schweitzer N M, Stucky G D, Marks L D, et al. Identification of active sites in CO oxidation and water-gas shift over supported Pt catalysts. Science. 2015 Oct 9; 350 (6257): 189 -192.
5. Salih, E. Y., Bashir, M. B. A., Rajpar, A. H., & Badruddin, I. A. (2022). Fabrication and characterization of porous Si/CuO film for visible light MSM photodetector: The effect of post-processing temperature. Ceramics International, 48(7), 9965-9972.
6. Salleh F, Usop R, Saugi N S, Salih E Y, Mohamad M, Ikeda H, et al. Influence of TiO2 layer's nanostructure on its thermoelectric power factor. Appl Surf Sci. 2019; 497: 143736 -1-5.
7. Bashir, M. B. A., Salih, E. Y., Rajpar, A. H., Bahmanrokh, G., & Sabri, M. F. M. (2022). The impact of laser energy on the photoresponsive characteristics of CdO/Si visible light photodetector. *Journal of Micromechanics and Microengineering*, *32*(8), 085006.
8. Abbas N K, Al-Attraqchi A A , Taha J H. Antimicrobial Activities of Green Biosynthesized Iron Oxide Nanoparticles Using F. Carica Fruit Extract. Indian J Forensic Med. 2020; april 14 (2) : 2181-2187.
9. Castro L, Blázquez M L, González F, Muñoz J Á, Ballester A. Biosynthesis of silver and platinum nanoparticles using orange peel extract: characterisation and applications. IET nanobiotechnology. 2015; 9: 252-258.
10. Mishra A, Mishra S, Manav N, Saluja D, Chandra R, Kaushik N. Synthesis, characterization, antibacterial and cytotoxic study of platinum (IV) complexes. Bioorg Med Chem. 2006; 14: 6333-6340.
11. Manav N, Mishra A, Kaushik N. In vitro antitumour and antibacterial studies of some Pt (IV) dithiocarbamate complexes. Spectrochim Acta Part A Mol Biomol Spectrosc. 2006; 65(1): 32-35.
12. Ruiz A L, Garcia C B, Gallón S N, Webster T J. Novel Silver-Platinum Nanoparticles for Anticancer and Antimicrobial Applications. Int J Nanomed. 2020; 15: 169–179.
13. Jabir N R, Tabrez S, Ashraf G M, Shakil S, Damanhouri G A, Kamal M A. Nanotechnology-based approaches in anticancer research. Int J Nanomed. 2012; 7: 4391-4408
14. Elhusseiny A F, Hassan H H. Antimicrobial and antitumor activity of platinum and palladium complexes of novel spherical aramides nanoparticles containing flexibilizing linkages: Structure–property relationship, Spectrochim Acta Part A Mol Biomol Spectrosc. 2013; 103: 232-245.
15. Yamada M, Foote M, Prow T W. Therapeutic gold, silver, and platinum nanoparticles, Wiley Interdisciplinary: Rev Nanomed Nanobiotechnol. 2015; 7 (3): 428-445.
16. Cho K H, Park J E, Osaka T, Park S G. The study of antimicrobial activity and preservative effects of nanosilver ingredient, Electrochim Acta. 2005; 51 (5): 956-960.
17. Kwon Y E, Whang K J, Park Y J, Kim K H. Synthesis, characterization and antitumor activity of novel octahedral Pt (IV) complexes. Bioorg Med Chem. 2003; 11: 1669-1676.
18. Liu X, Zhang J, Yang T, Guo X, Wu S, Wang S. Synthesis of Pt nanoparticles functionalized WO3 nanorods and their gas sensing properties. Sens Actuators B Chem. 2011; 156: 918-923.
19. Mishra A, Kaushik N. Synthesis, characterization, cytotoxicity, antibacterial and antifungal evaluation of some new platinum (IV) and palladium (II) complexes of thiodiamines, Eur J Med Chem. 2007; Oct 42(10): 1239-1246.
20. Öğütçü H, Yetim N K, Özkan E H, Eren O, Kaya G, Sarı N, et al. Nanospheres caped Pt (II) and Pt (IV): synthesis and evaluation as antimicrobial and Antifungal Agent. Pol J Chem Technol. 2017; 19 (1): 74-80.
21. Sharma K D. Antifungal activity of biogenic platinum nanoparticles: an in vitro study. Int J Curr Microbiol App Sci. 2017; 6(4): 334-340.
22. Velmurugan P, Shim J, Kim K, Oh B T. Prunus× yedoensis tree gum mediated synthesis of platinum nanoparticles with antifungal activity against phytopathogens. Mater Lett. 2016; 174: 61-65.
23. Das S K, Dickinson C, Lafir F, Brougham D F, Marsili E. Synthesis, characterization and catalytic activity of gold nanoparticles biosynthesized with Rhizopus oryzae protein extract. Green Chem. 2012; 14: 1322-1334.
24. Konishi Y, Ohno K, Saitoh N, Nomura T, Nagamine S, Hishida H, Takahashi Y, Uruga T. Bioreductive deposition of platinum nanoparticles on the bacterium Shewanella algae. J. Biotechnol. 2007; 128 (3): 648-653.
25. Kumar B, Smita K, Cumbal L, Debut A. Ficus carica (Fig) fruit mediated green synthesis of silver nanoparticles and its antioxidant activity: a comparison of thermal and ultrasonication approach. Bio Nano Science. 2016; 6: 15-21.

2023, 20(3 Suppl.): 1146- 1154
https://dx.doi.org/10.21123/bsj.2023.7294
P-ISSN: 2078-8665 - E-ISSN: 2411-7986
Baghdad Science Journal

26. Perez C, Pauli M, Bazerque P. Antibiotic assay by agar-well diffusion method. Acta Biol Med Exp. 1990; 15: 113-115.
27. Syed A, Ahmad A. Extracellular biosynthesis of platinum nanoparticles using the fungus Fusarium oxysporum. Colloids Surf B Biointerfaces. 2012; Sep 97 (1): 27-31.
28. Shah M. Growth of uniform nanoparticles of platinum by an economical approach at relatively low temperature. Sci Iran. 2012; 19 (3): 964-966.
29. Bashir, M. B. A., Salih, E. Y., Sabri, M. F. M., Rajpar, A. H., Badruddin, I. A., Hussein, M. Z., & Al-Jumaili, B. E. (2021). In-depth thermal, microstructural and photoluminescence analysis of mesoporous ZnO/ZnAl2O4-MMO: the effect of molar ratio. *ECS Journal of Solid State Science and Technology*, *10*(10), 106006.
30. Salih, E. Y., Ramizy, A., Aldaghri, O., Mohd Sabri, M. F., Madkhali, N., Alinad, T., ... & Eisa, M. H. (2022). In-depth optical analysis of Zn (Al) O mixed metal oxide film-based Zn/Al-layered double hydroxide for TCO application. *Crystals*, *12*(1), 79..
31. Balouch A, Ali Umar A, Mawarnis E R, Saad S K M, Mat Salleh M, Abd Rahman M Y, Kityk I, Oyama M. Synthesis of amorphous platinum nanofibers directly on an ITO substrate and its heterogeneous catalytic hydrogenation characterization. ACS Appl Mater Interfaces. 2015; 7 (14): 7776–7785.
32. Thirumurugan A, Aswitha P, Kiruthika C, Nagarajan S, Christy A N. Green synthesis of platinum nanoparticles using Azadirachta indica–An eco-friendly approach. Mater Lett. 2016; 170 (2016): 175-178.
33. Salih, E. Y., Ramizy, A., Aldaghri, O., Sabri, M. F. M., Madkhali, N., Alinad, T., ... & Eisa, M. H. (2022). Rapid Synthesis of Hexagonal-Shaped Zn (Al) O-MMO Nanorods for Dye-Sensitized Solar Cell Using Zn/Al-LDH as Precursor. *Nanomaterials*, *12*(9), 1477..
34. Soomro R A, Sherazi S H, Memon N, Shah M, Kalwar N, Hallam K R, Shah A. Synthesis of air stable copper nanoparticles and their use in catalysis, Adv Mater Lett. 2014; 5 (4): 191-198.
35. Warris A, Verweij P. Clinical implications of environmental sources for Aspergillus. Med Mycol. 2005; 43 (1): S59-S65.
36. Klis F M, de Koster C G, Brul S. Cell wall-related bionumbers and bioestimates of Saccharomyces cerevisiae and Candida albicans. Eukaryotic cell.2014; 13 (1): 2-9.

تصنيع جزيئات البلاتين النانوية باستخدام مستخلص فاكهة تين الكاريكا وتقييم نشاطها المضادة للميكروبات

جنان حسين طه [1]، ندى خضير عباس [2] و أزهار عبد الفتاح الأطرقجي [3]

[1]قسم الفسلجة والفيزياء الطبية ، كلية الطب، جامعة النهرين ، بغداد ، العراق.
[2]-قسم الفيزياء ، كلية العلوم للبنات، جامعة بغداد، بغداد ، العراق.
[3]-قسم الأحياء الدقيقة، كلية الطب، جامعة النهرين، بغداد، العراق.

الخلاصة

في هذا البحث، تم التوصل لطريقة جديدة بسيطة للتخليق الأخضر لجسيمات البلاتين النانوي (Pt NPs) باستخدام مستخلص التين. في الوقت نفسه، تم فحص خواص هيكل والمورفولوجيا لـ لجسيمات البلاتين النانوي المُصنَّع بدقة. على وجه الخصوص، أظهرت جسيمات البلاتين النانوية (Pt NPs) التي تم الحصول عليها شكلًا كرويًا بمدى قطر يبلغ 5-30 نانومتر ومتوسط جذر يبلغ 9.48 نانومتر باستخدام مجهر النافذ الإلكتروني (TEM) ومجهر القوة الذري (AFM)، على التوالي. بالإضافة إلى ذلك، تم فحص المنتج النهائي لجسيمات البلاتين النانوية (Pt NPs) كعامل مضاد للفطريات ومضاد للبكتيريا ضد نوعين Candida وAspergillus بالإضافة إلى Staphyllococcus aureus موجبة الجرام وAcinetobacter سالبة الجرام على التوالي. وفقًا لذلك، أظهرت البلاتين النانوي المُصنَّع مناطق تثبيط تبلغ 36 ملم و28 ملم ضد الأنواع الفطرية والبكتيرية، على التوالي. تلعب جسيمات البلاتين النانوية المقدمة دورًا نشطًا في كل من الأنشطة المضادة للفطريات والبكتيريا والتي تشير إلى وجود نظام مواد نانوية جيدًا للتطبيق الطبي الحيوي.

الكلمات المفتاحية: مضاد للجراثيم ، مضاد للفطريات ، مستخلص F. carica ، التوليف الأخضر ، Pt NPs.